# 2

# Supercapacitor-Based Electrical Energy Storage System

Masatoshi Uno
*Japan Aerospace Exploration Agency, Japan*

## 1. Introduction

Supercapacitors (SCs), also known as electric double-layer capacitors or ultracapacitors, are energy storage devices that store electrical energy without chemical reactions. Energy storage mechanisms that do not require chemical reactions provide several advantages over traditional secondary batteries such as lead-acid, Ni-Cd, Ni-MH and lithium-ion batteries (LIBs) in terms of cycle life performance, power capability, coulombic efficiency and low-temperature performance. In addition to these superior electrical properties, it is easier to estimate the state of charge (SoC) for SCs than that for secondary batteries because the terminal voltage of SCs is inherently proportional to the SoC.

In order to meet load variations, SCs are widely used as auxiliary power sources that complement main energy sources such as secondary batteries and fuel cells. In such applications, SCs act as electrical power buffers with large power capability. SCs are currently considered to be unsuitable as main energy storage sources because their specific energy values are lower than those of secondary batteries. However, with the emergence of new technologies and new chemistries that can lead to increased specific energies and reduced cost, they are considered to be attractive alternatives to main energy storage sources, especially because of their long life.

However, SCs have some major drawbacks originating from their inherent electrical properties. These are as follows:

1. The specific energy of SCs is lower than that of traditional secondary batteries.
2. Cell/module voltages of SCs in a series connection need to be eliminated since cell/module voltage imbalance may result in premature irreversible deteriorations and/or decrease in available energy.
3. Since the specific energy of SCs is low, energy stored by SCs should be delivered to loads as efficiently as possible in order to avoid energy wastage.
4. Terminal voltages of SCs vary widely with charging/discharging processes. Power converters having wide voltage ranges are required to power loads within a particular voltage range.

This chapter presents the SC-based electrical energy storage systems as alternatives to traditional battery-based systems. In the following sections, the above-mentioned issues are addressed in detail. In Section 2, the potential of SCs as alternative main energy storage sources is discussed on the basis of comparisons with specific energy and cycle life performance of a lithium-ion battery. In Section 3, cell/module voltage equalizers that are

operable with a single switch or even without switches are introduced and compared with conventional topologies in terms of the number of components. Section 4 presents high-efficiency power converters suitable for SCs.

## 2. Supercapacitors as main energy storage sources

In general, the specific energy of SCs is lower than that of traditional secondary batteries. For example, specific energies of lead-acid and alkaline batteries (such as Ni-Cd and Ni-MH batteries) are 20–40 and 40–80 Wh/kg, respectively, and those of LIBs are at least 150 Wh/kg. On the other hand, the specific energy of conventional SCs does not exceed 10 Wh/kg. Lithium-ion capacitors (LICs), which are newly emerging SCs having a new chemistry, offer values less than 30 Wh/kg, which are comparable to those of lead-acid batteries but remain lower than other battery chemistries. LICs can match lead-acid batteries but their costs are not comparable. Meanwhile, there is still a large gap between LIBs and SCs (including LICs) in terms of specific energy, and therefore, SCs are usually considered unsuitable as main energy storage sources. However, SCs are considered to be potential alternative main energy storage sources considering their net specific energy, which is defined as

$$\text{Net Specific Energy} = \text{Specific Energy} \times \text{Depth of Discharge}, \tag{1}$$

as well as their cycle life performance. For example, in low-Earth orbit satellite applications, where a minimum service life of three years is required for energy storage systems, three types of energy storage sources, (i) alkaline batteries, (ii) LIBs and (iii) SCs, are compared in terms of specific energy, depth of discharge (DoD) and net specific energy. The comparisons are shown in Table 1. Traditional secondary batteries for such satellites are operated with relatively shallow DoD of 20%–25%, allowing the life requirement to be fulfilled. Therefore, the net specific energies of alkaline batteries are 8–20 Wh/kg, and similarly, those of LIBs are 30–50 Wh/kg, although LIBs offer high specific energies of 150–200 Wh/kg. On the other hand, SCs can be cycled with deep DoD values even for such long-term applications because their cycle life performance is inherently excellent and is independent on DoD (as shown later). For LICs, the net specific energy reaches <24 Wh/kg for a DoD of 80% and the gap between secondary batteries and SCs (especially LICs) can, therefore, be bridged.

| | Alkaline Battery (Ni-Cd, Ni-MH) | LIB | Supercapactor | |
|---|---|---|---|---|
| | | | Conventional | LIC |
| Specific Energy | 40–80 Wh/kg | 150–200 Wh/kg | < 10 Wh/kg | < 30 Wh/kg |
| Depth of Dischar | 20–25% | 20–25% | < 80% | < 80% |
| Net Specific Ener | 8–20 Wh/kg | 30–50 Wh/kg | < 8 Wh/kg | < 24 Wh/kg |

Table 1. Specific energy, depth of discharge and net specific energy for traditional secondary batteries and SCs for low-Earth orbit satellite applications.

Fig. 1 shows an example of cycle life performance test results for a 3-Ah-class LIB and 2000-F-class LICs cycled with 20% and 80% (40%) DoD, respectively, at 25°C. A single cycle consists of a 65-min charge and 35-min discharge, and 10000 cycles are equivalent to approximately 1.9 years of service. The LIB deteriorated by 30% at the 10000th cycle while the LICs retained more than 96% of their initial capacitance, as shown in Fig. 1(a). The

degradation of the LICs was almost independent on DoD, although that of LIBs, in general, significantly depends on DoD (Yoshida, et al., 2010). The deeper the DoD, the greater will be the deterioration experienced by the LIBs. Fig. 1(b) shows cycle life performance as a function of the square root of cycle number, using which the cycle life performance can be depicted linearly. The cycle life performances of the LIB and LICs can be predicted by extrapolating with straight lines (Mita, et al., 2010). The capacitance retention is expressed as a function of number of cycles and is expressed as

$$\text{Capacitance Retention} = 100 - K \times (\text{Number of Cycles})^{0.5} \quad (2)$$

where $K$ is the degradation rate constant. From the results shown in Fig. 1(b), the values of $K$ for the LIB and LICs were calculated to be 0.3 and 0.04, respectively. From Eq. (1), the cycle life of LIC is expected to be approximately 56 times longer than that of LIB under a given condition. For the LIB to achieve a cycle life that is as long as that of the LIC, the DoD must be shallower in order to alleviate degradations due to cycling. However, a lower DoD also results in a decrease in the net specific energy of the LIB, as determined by Eq. (1). Thus, from two aspects, the net specific energy and the cycle life performance, SCs (especially LICs) can be used as main energy storage sources and are suitable alternatives to traditional secondary batteries for shallow DoD applications.

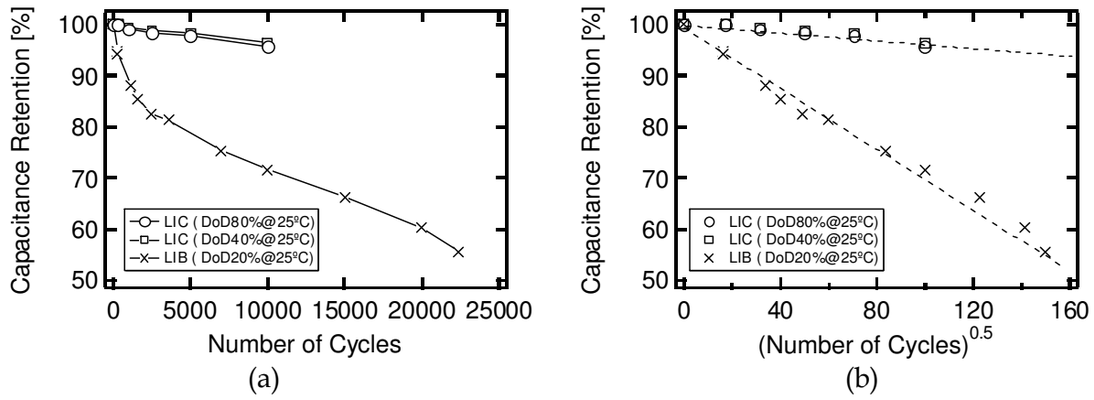


Fig. 1. Cycle life performances of a lithium-ion battery and lithium-ion capacitors as a function of (a) number of cycles and (b) square root of number of cycles.

The above comparison focuses on alternative applications for the batteries with shallow DoD for long-term cycle life. However, for deep DoD applications where the batteries are almost fully discharged, SCs cannot match the batteries from the perspective of net specific energy and cannot be an alternative energy storage source. Thus, SCs are practical and most suitable as main energy storage sources for applications where the batteries are used with shallow DoDs to achieve long cycle lives.

## 3. Cell/module voltage equalizer

### 3.1 Conventional cell/module voltage equalizer

Cell/module voltage equalizers are commonly used for SCs and LIBs. Voltage imbalances among cells/modules may result in not only reduced available energy but also premature deterioration caused by overcharging and over-discharging. In this section, representative

conventional cell/module voltage equalizers are presented and technical concerns regarding their circuit complexity and reliability are addressed.

Various cell voltage equalizers, including dissipative and nondissipative approaches, have been proposed, demonstrated and reviewed (Cao, et al., 2008; Guo, et al., 2006). Fig. 2 shows the basic topologies of four examples of conventional dissipative and nondissipative equalizers. Various derivatives have also been proposed but are not shown here. As discussed in Section 2, the specific energy of SCs is lower than that of LIBs, so a larger number of cells/modules may be needed to constitute an SC-based energy storage system. The greater the number of cells/modules connected in series, the greater will be the number of voltage equalizers required. However, the system's complexity is prone to increase as the number of voltage equalizers increases, and hence, simple equalizers are desirable for SC-based energy storage systems.

The most prevalent topology is a shunting equalizer (Fig. 2(a)) (Isaacson, et al., 2001; Uno, 2009) that is a dissipative equalizer. Several battery management ICs containing dissipative equalizers are currently available. Dissipative equalizers typically consist of a series combination of a transistor and a current-limiting resistor. Excess stored energies of cells or charge currents are shunted to the transistor and resistor when the cell voltage exceeds a certain value. In other words, the excess energy or charge current is dissipated at the transistor and resistor, and this process generates heat, which is not desirable as it negatively impacts the energy efficiency and thermal management of the system.

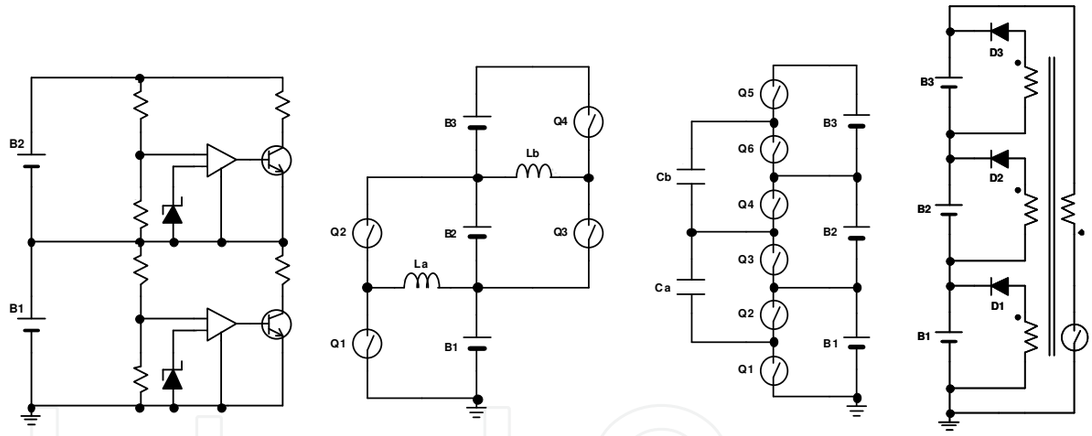


Fig. 2. Conventional cell/module voltage equalizers: (a) shunting equalizer, (b) buck-boost converter equalizer, (c) switched capacitor converter equalizer and (d) multi-winding flyback-based equalizer.

Conventional nondissipative equalizers are typically based on multiple individual dc–dc converters such as buck-boost converters (Nishijima, et al., 2000) and switched capacitor converters (Pascual & Krein, 1997), as shown in Figs. 2(b) and (c), respectively. In these topologies, the charges or energies of the series-connected cells can be exchanged between adjacent cells to eliminate cell voltage imbalance.

In the equalizers shown in Figs. 2(a), (b) and (c), the number of switches needed is proportional to the number of series connections of the cells. The number of switches is a good index for representing a circuit's complexity because switches require drivers and/or ancillary components. Hence, the circuit complexity and cost are prone to increase as the

number of series connections increases, especially for applications where numerous series connections of cells are necessary.

In a transformer-based equalizer incorporating flyback- and forward-based topologies, the energies of series-connected cells can be redistributed via a multi-winding transformer (Kutkut, et al., 1995) to the cell having the lowest voltage. Fig. 2(d) depicts the flyback-based equalizer. The number of switches required are significantly less than those required with other topologies. However, this topology needs a multi-winding transformer that must be customized according to the number of series connections, and hence, the modularity is not good. In addition, the design and parameter matching for multiple windings are considered difficult (Cao et al., 2008).

As mentioned in Section 2, the specific energy of SCs is lower than that of traditional secondary batteries, so an SC-based energy storage system may require a larger number of cells to be connected in series and/or parallel than secondary batteries, although SCs have potentials to match or outperform the traditional batteries in terms of net specific energy for particular applications. In other words, the number of series connections of SCs is prone to be larger than that of secondary batteries. Hence, using multiple switches or transformer windings, which leads to increased cost and circuit complexity, is undesirable for an SC-based energy storage system. In addition, conventional topologies are undesirable because of their complexity, since electrical circuits should be as simple as possible in order to mitigate risks of failure, especially for applications that require long-term use, i.e., SC-based energy storage systems.

### 3.2 Voltage equalizer using single-switch multi-stacked SEPICs

#### 3.2.1 Circuit configuration and major benefits

Fig. 3 shows a single-switch cell/module voltage equalizer for four series-connected SCs. This topology operates as a charger with an equalization function. $V_{in}$ is the external power source, and the circuit consisting of $V_{in}$, $C_{in}$, $L_{in}$, Q, $C_1$, $L_1$, $D_1$ and $SC_1$ is identical to a conventional single ended primary inductor converter (SEPIC). The circuits consisting of $C_i$-$D_i$-$L_i$ (i = 1…4) are identical and multi-stacked; inductor–diode pairs are stacked in series while all the capacitors are connected to Q and $L_{in}$. Hence, this equalizer may be regarded as a multi-stacked SEPIC.

This circuit contains a single active device (i.e., switch) and multiple passive components. This single-switch circuit configuration contributes to a significant reduction in circuit complexity when compared to the conventional topologies illustrated in Fig. 2. This equalizer is also advantageous with regards to its drive circuits. The conventional topologies shown in Figs. 2(b) and (c) require floating gate drivers in cases where N-channel MOSFETs are used for high-side switches (even-numbered switches in Figs. 2(b) and (c)). The equalizer shown in Fig. 3, on the other hand, does not require a floating gate drive circuit because the switch is connected to the ground. Moreover, since the basic topology of this equalizer is SEPIC, commercially available control ICs for SEPICs can be employed. Therefore, this equalizer reduces not only the number of switches but also the complexity of the gate drive circuit. Furthermore, this equalizer also offers good modularity because the number of series connections can be arbitrarily extended by stacking the circuit of $C_i$-$D_i$-$L_i$, without the need for additional active components such as switches or control ICs.

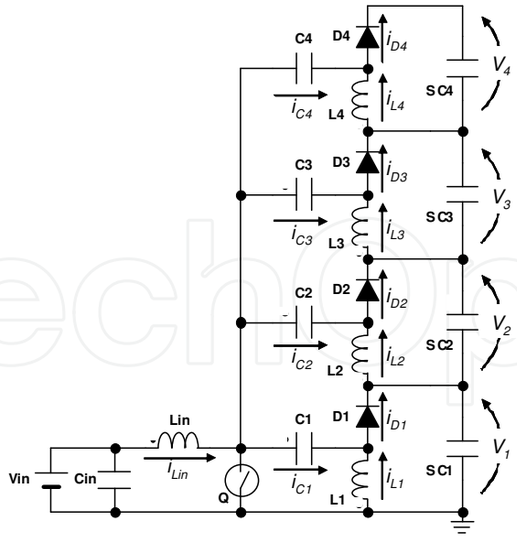


Fig. 3. Single-switch cell/module voltage equalizer using multi-stacked SEPICs.

### 3.2.2 Fundamental operation

The fundamental operation of this equalizer is similar to that of a conventional SEPIC. Fig. 4 shows the theoretical operating waveforms and current flow directions. When the switch is turned on ($T_{on}$ period), all the inductor currents increase and the corresponding energies are stored in each inductor. When the switch is tuned off ($T_{off}$ period), the diodes are turned on and all the inductor currents decrease. The current in $L_{in}$ is distributed to each capacitor and SC depending on each cell voltage. As long as the cell voltages are uniform and cell impedances are negligible, the current in $L_{in}$ is uniformly distributed to each capacitor.

The average voltage of inductors under a steady-state condition is zero. The voltages of the capacitors $C_1$–$C_4$, referred to as $V_{C1}$–$V_{C4}$, respectively, are

$$\begin{cases} V_{C1} = V_{in} \\ V_{C2} = V_{in} - V_1 \\ V_{C3} = V_{in} - (V_1 + V_2) \\ V_{C4} = V_{in} - (V_1 + V_2 + V_3) \end{cases} \tag{3}$$

where $V_{in}$ is the input voltage and $V_1$–$V_4$ are voltages across $SC_1$–$SC_4$ denoted in Fig. 3, respectively. The voltage–time product of inductors in a single cycle under a steady-state condition is also zero. Therefore,

$$\begin{cases} DV_{C1} & = (1-D)(V_1 + V_{D1}) \\ D(V_{C2} + V_1) & = (1-D)(V_2 + V_{D2}) \\ D(V_{C3} + V_1 + V_2) & = (1-D)(V_3 + V_{D3}) \\ D(V_{C4} + V_1 + V_2 + V_3) & = (1-D)(V_4 + V_{D4}) \end{cases} \tag{4}$$

where $D$ is the duty cycle and $V_{D1}$–$V_{D4}$ are forward voltages of $D_1$–$D_4$, respectively. From Eqs. (3) and (4), we get

$$V_i = \frac{D}{1-D} V_{in} - V_{Di} \tag{5}$$

Eq. (5) indicates that this equalizer outputs uniform voltages to all SCs as long as the diodes' forward voltages are uniform. In the case where cell voltages are imbalanced, $D$ can be controlled in order to regulate the output voltages higher and lower than the lowest and other SC voltages, respectively. This allows the cell having the lowest voltage to be charged preferentially.

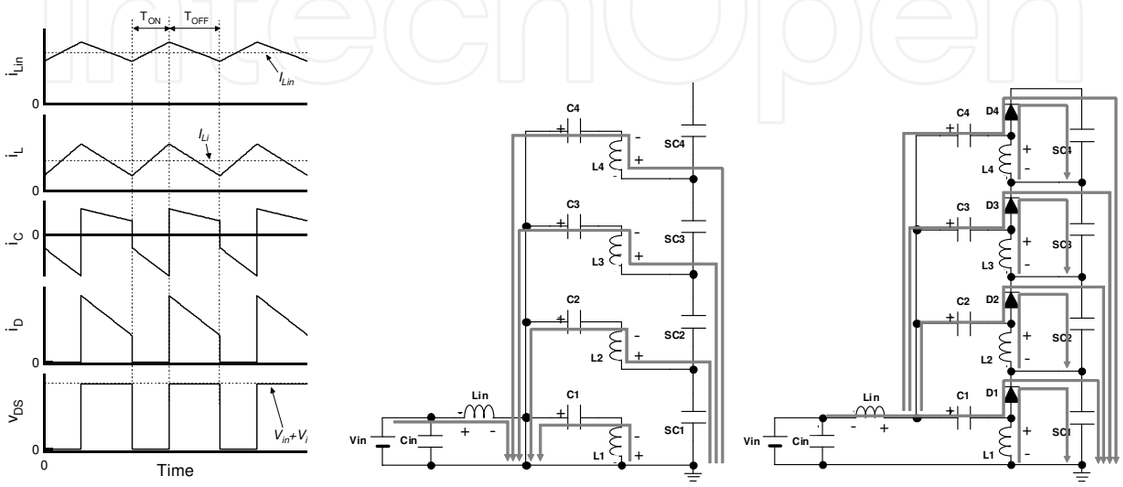


(a) (b) (c)

Fig. 4. (a) Theoretical operating waveforms and current directions during (b) $T_{on}$ and (c) $T_{off}$.

### 3.2.3 Experimental equalization performance

Four SC modules with capacitance of 220 F each were connected in series and charged from an initially voltage-imbalanced condition by using a 40 W prototype shown in Fig. 5(a).The voltage input to the equalizer was 28 V, and by employing PWM control using a switching regulator IC (LTC1624) operating at 200 kHz, the input current and charge voltage were regulated to be 1.5 A and 14.5 V, respectively.

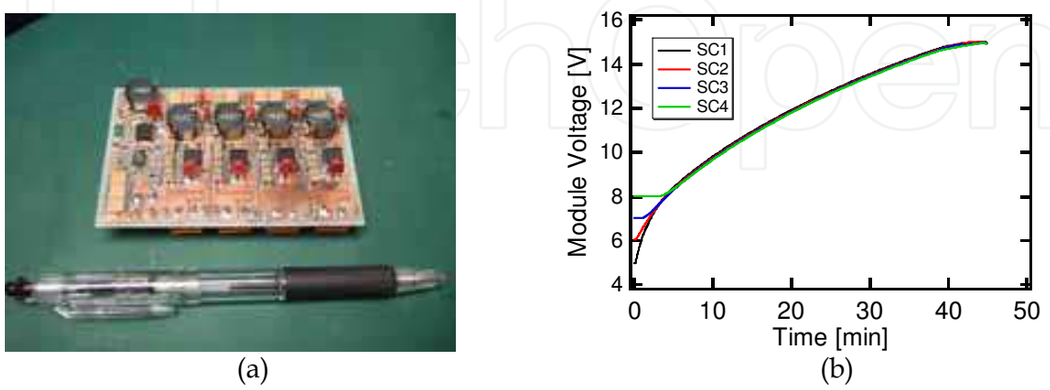


(a) (b)

Fig. 5. (a) Photograph of the 40 W prototype of the equalizer using multi-stacked SEPICs, and (b) experimental charge profiles of four series-connected SC modules charged by the prototype from an initially voltage-imbalanced condition.

The SC module(s) having the lowest voltage was(were) charged preferentially at each instant and the voltage imbalance was eliminated as the charging progressed, as shown in Fig. 5(b). After the voltage imbalance was eliminated, all the SC voltages increased uniformly. Eventually, at the end of the charge, all the SCs was charged to the uniform voltage of 14.5 V.

### 3.3 Switchless voltage equalizer

#### 3.3.1 Circuit configuration and major benefits

A switchless voltage equalizer for three series-connected SCs is shown in Fig. 6. This topology also operates as a charger with an equalization function; the charge is provided by an ac power source. Two series-stacked diodes are connected to each SC and the junctions of stacked diodes are connected to the ac power source via energy transfer capacitors $C_1$–$C_3$.

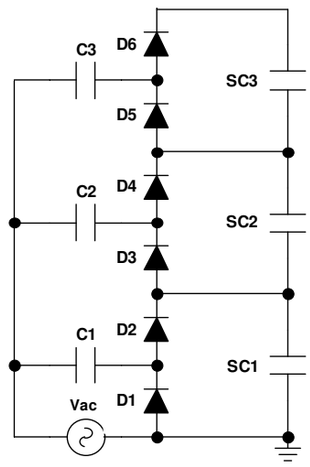


Fig. 6. Switchless cell/module voltage equalizer.

This equalizer consists of passive components only, resulting in reduced circuit complexity and improved equalizer reliability when compared with those of conventional ones. Similar to the single-switch equalizer presented in the previous section, this equalizer also exhibits good modularity. The number of series-connected SCs can be easily extended by adding a capacitor and stacked diodes.

#### 3.3.2 Fundamental operation

The equalizer operates in two modes, and the current flow direction in each mode is shown in Fig. 7. Each SC can be charged to a uniform voltage level by the ac power source while alternating between the two modes.

In mode A, odd-numbered diodes are turned on and $C_1$–$C_3$ are charged by the ac power source and $SC_1$–$SC_2$. The voltages of $C_1$–$C_3$ in mode A are $V_{C1A}$–$V_{C3A}$, respectively, and are given by

$$\begin{cases} V_{C1A} = E_A - V_D \\ V_{C2A} = E_A + V_{SC1} - V_D \\ V_{C3A} = E_A + V_{SC1} + V_{SC2} - V_D \end{cases} \tag{6}$$

where $E_A$ is the peak voltage of the ac power source in mode A and $V_D$ is the forward voltage of the diodes.

In mode B, $C_1$–$C_3$ discharge to the SCs via even-numbered diodes and the voltages of $C_1$–$C_3$ in mode B are $V_{C1B}$–$V_{C3B}$, respectively, and are given by

$$\begin{cases} V_{C1B} = E_B + V_{SC1} + V_D \\ V_{C2B} = E_B + V_{SC1} + V_{SC2} + V_D \\ V_{C3B} = E_B + V_{SC1} + V_{SC2} + V_{SC3} + V_D \end{cases} \quad (7)$$

where $E_B$ is the bottom voltage of the ac power source in mode B.
In general, the average current through capacitor, $I_{Ci}$, is given by

$$I_{Ci} = C_i \times f \times \Delta V_{Ci} \quad (8)$$

where $C_i$ is the capacitance of $C_i$ (i = 1…3), $f$ is the frequency and $\Delta V_{Ci}$ is the voltage variation across $C_i$. $\Delta V_{Ci}$ is obtained by subtracting Eq. (7) from Eq. (6). Substituting the result into Eq. (8) gives

$$I_{Ci} = C_i f \left\{ \left( E_A - E_B \right) - 2V_D - V_{SCi} \right\} \quad (9)$$

($E_A$ − $E_B$) is equivalent to the peak-to-peak voltage of the ac power source. This equation implies that all the SCs are charged to the uniform voltage level of ($E_A$ − $E_B$) − $2V_D$ at the end of the charge at which $I_{Ci}$ becomes zero. The charge rate is determined by $C_if$ whose dimension is the inverse of resistance (i.e., conductance). The greater the capacitance of $C_i$ and $f$, the quicker the SCs will be charged. The inverse of $C_if$, $R_{Cf}$, can be used as an index to represent the charging speed.

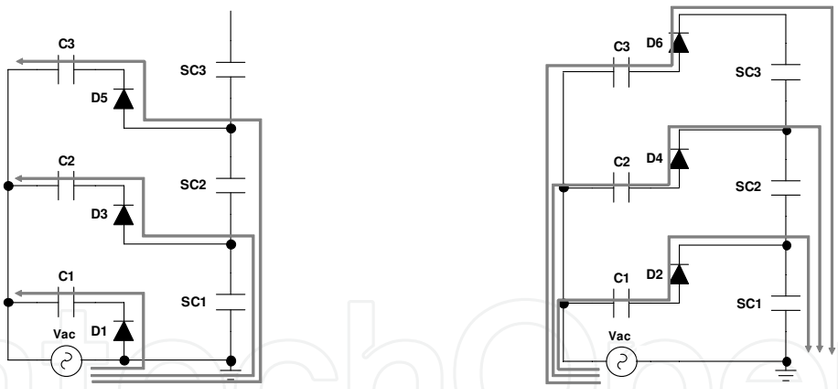


Fig. 7. Current flow directions in (a) mode A and (b) mode B.

### 3.3.3 Experimental equalization performance

Three SC modules with capacitance of 60 F each were connected in series and charged from an initially voltage-imbalanced condition using a prototype with $R_{Cf}$ of 42 Ω (Fig. 8(a)). Al electrolytic capacitors having capacitance of 470 μF each were used for $C_1$–$C_3$. The ac voltage for the equalizer was 17 Vac (peak-to-peak voltage of 48 V) and was provided by a 50 Hz utility power source via a transformer.
The SC modules were charged at different charge rates, as indicated by Eq. (9), and are shown in Fig. 8(b). The voltage imbalance was gradually eliminated as the charging progressed. Eventually, all the SCs were charged to a uniform voltage of approximately 47

V, which is 1 V lower than the peak-to-peak voltage of the ac power source. This difference is attributed to diode voltage losses.

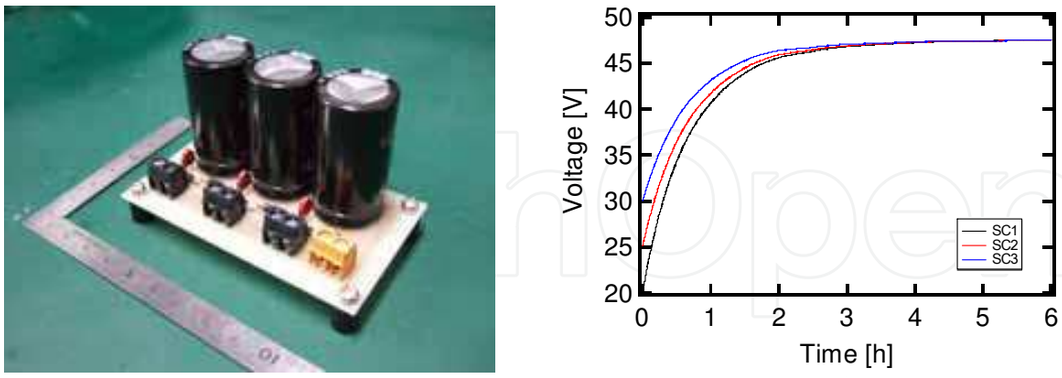


(a) (b)

Fig. 8. (a) Photograph of the prototype of the switchless equalizer, and (b) experimental charge profiles of three series-connected SC modules charged by the prototype from an initially voltage-imbalanced condition.

### 3.4 Comparison for circuit complexity and number of components

In Table 2, two topologies presented in the previous sections are compared with the conventional equalizers. As mentioned in Section 3.1, the number of switches is a good index for representing a circuit's complexity. The number of switches required for conventional equalizers such as shunting, buck-boost and switched capacitor equalizers is proportional to the number of series-connected cells/modules, $n$. The transformer-based (flyback) equalizer can operate with a single switch, but the need for $(n + 1)$ windings results in poor modularity, design difficulties and cost penalty. However, the two topologies described in previous sections require neither multiple switches nor transformer windings, although they require multiple passive components. Therefore, these topologies have advantages over conventional ones in terms of circuit complexity, modularity and cost, especially for applications where numerous series connections of cells/modules are necessary. Moreover, employing fewer active components leads to reduced risks of failure and improved reliability.

These topologies can be applied for both SCs and LIBs.

| Topology | Switch | R | L | C | D | Transformer |
|---|---|---|---|---|---|---|
| Multi-Stacked SEPICs | 1 | - | $n$ + 1 | $n$ | $n$ | - |
| Switchless Equalizer | - | - | - | $n$ | $2n$ | 1 (1 core with 2 windings) |
| Shunting Equalizer | $n$ | $n$ | - | - | - | - |
| Buck-Boost | $2n$ - 1 | - | $n$ - 1 | - | - | - |
| Switched Capacitor | $2n$ | - | - | $n$ - 1 | - | - |
| Transformer (Flyback) | 1 | - | - | - | $n$ | 1 (1 core with $(n$ + 1) windings) |

(Smoothing capacitor is excluded)

Table 2. Comparison of the number of components required for each equalizer.

## 4. High-efficiency power converters with wide voltage range

### 4.1 Conventional power converters

As discussed in Section 1, power converters in SC-based energy storage systems are required to operate over a wide voltage range because SC voltages vary significantly due to charge–discharge processes. For the SC-based electrical energy storage systems as alternatives to traditional battery-based systems, the converters need to operate over a wide input voltage range and provide power to loads within a voltage range that is at least comparable to battery voltage variations. In addition, the power converters should operate as efficiently as possible. With traditional switching power converters, the stored energies of SCs can be provided to loads at a constant voltage, and the SCs can be discharged sufficiently deep. However, designing traditional converters to operate over a wide voltage range leads to increase and decrease in size and efficiency, respectively. An increase in the size of magnetic components such as inductors and transformers, which are relatively large components in converters, is significant. Since available energies of SCs are proportional to the converter efficiency, a decrease in the converter efficiency results in either a decrease in available energy or an increase in size, weight and cost of SCs.

Although emphasis on chargers is necessary, this section focuses on dischargers, which are especially important for SC-based energy storage systems, because the energy requirement as well as size and weight of SCs are directly proportional to the discharger efficiency.

### 4.2 Discharger using cascaded switched capacitor converters with selectable intermediate taps

#### 4.2.1 Conventional switched capacitor converter and conceptual derivation of cascaded switched capacitor converters with selectable intermediate taps

Switched capacitor converters (SCCs) that do not require magnetic components have been proposed for non-isolated intermediate bus converters and automotive applications (Oraw & Ayyanar, 2007; Peng, et al., 2003; Xu, et al., 2006). SCCs achieve both high efficiency and high power density, but their input–output voltage ratio is usually uncontrollable and is a fixed value that is determined by the number of capacitors stacked in series.

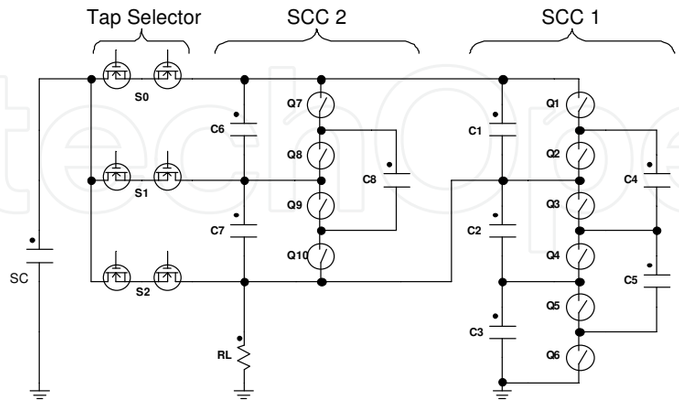


Fig. 9. SC Discharger using cascaded switched capacitor converters with selectable intermediate taps.

SCCs operate as nondissipative voltage dividers that produce $M$ discrete voltage levels when $M$ capacitors are stacked in series. In other words, voltage levels that can be provided

by SCCs to a load that incorporates an SC having a voltage of $V_{SC}$ are $V_{SC}(1/M)$, $V_{SC}(2/M)$ …$V_{SC}$. As $V_{SC}$ varies with charge-discharge processes, these voltage levels also vary. However, by selecting one of these voltage levels in accordance with the variation in $V_{SC}$, the load voltage can be maintained within a desired voltage range.
On the basis of the concept of selecting one of the multiple voltage levels, SCCs having selectable intermediate taps are derived as shown in Fig. 9. Two SCCs, referred to as SCCs 1 and 2, are cascaded to produce fine discrete voltage levels, and selectable intermediate taps are connected between SC and SCC 2. The SC voltage is divided via two stages using two SCCs, and the load voltage can be maintained by selecting one of the intermediate taps.

### 4.2.2 Operating principle

Each SCC consists of switches, stationary capacitors ($C_1$–$C_3$ and $C_6$–$C_7$) and energy transfer capacitors ($C_4$–$C_5$ and $C_8$). Odd- and even-numberd switches in each SCC alternate with a duty cycle of almost 50% to transfer charges among capacitors. Ideally, the capacitor voltages in each SCC become uniform. The load is directly connected to $C_2$–$C_3$ in SCC 1, and SCC 2 is cascaded to SCC 1 via $C_1$. The relationship between the load voltages ($V_{Load}$) and the capacitors in SCC 1 and SCC 2, ($V_{C1}$ and $V_{C2}$), is given by

$$V_{Load} = 2V_{C1} = 4V_{C2} \tag{10}$$

One of the intermediate taps (MOSFET relays $S_0$–$S_2$) is selected accordingly, and $V_{SC}$ is equal to the voltage level of the selected intermediate tap. For example, when $S_0$ is on, $V_{SC}$ is the sum of the voltages across $C_6$–$C_7$ and $V_{Load}$. On the other hand, when $S_1$ is on, $V_{SC}$ is the sum of the voltages across $C_7$ and $V_{Load}$. Therefore, the relationship between $V_{SC}$ and $V_{Load}$ can be generalized as

$$V_{Load} = \frac{4V_{SC}}{6 - N} \tag{11}$$

where $N$ is the subscript of $S_0$–$S_2$.

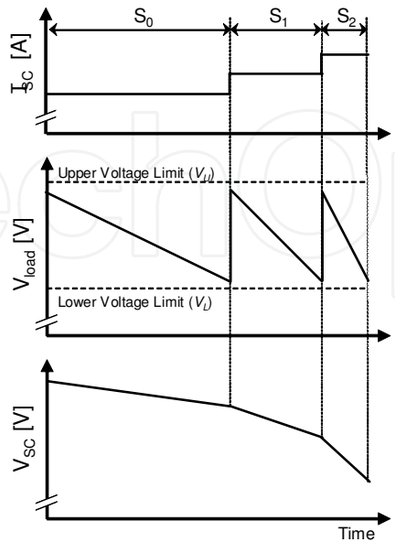


Fig. 10. Discharge characteristics of an SC with the discharger using cascaded switched capacitor converters with selectable intermediate taps.

The discharging characteristics of an SC when using the discharger shown in Fig. 9 are illustrated in Fig. 10. At the beginning of the discharging process of the SC, $S_0$ is turned on and the SC discharges via $S_0$ to the SCCs. $V_{Load}$ is four-sixth of $V_{SC}$, as determined by Eq. (11). By assuming that the SCCs operate ideally without power conversion losses, the SC current, $I_{SC}$, is four-sixth of the load current, $I_{Load}$. As discharging progresses, $V_{Load}$ and $V_{SC}$ decrease. When $V_{Load}$ decreases to the lower voltage limit level, $V_L$, $S_0$ and $S_1$ are turned off and on, respectively, in order to raise $V_{Load}$. After $S_1$ is turned on, $V_{Load}$ increases to four-fifth of $V_{SC}$. Simultaneously, $I_{SC}$ also increases to four-fifth of $I_{Load}$. The gradient of $V_{SC}$ during $S_1$-on period becomes steeper than that during $S_0$-on period because of the larger $I_{SC}$. With further discharging, $V_{Load}$ decreases further until it reaches $V_L$ again. Then, $S_2$ is turned on in order to raise $V_{Load}$ again. During $S_2$-on period, $V_{Load}$ and $I_{Load}$ are equal to $V_{SC}$ and $I_{SC}$, respectively, because the load and SC are connected directly via $S_2$. Stepwise increases in $I_{SC}$ result in inflection points in $V_{SC}$.

The above-mentioned sequence is repeated to maintain $V_{Load}$ within a desired voltage range bounded by upper and lower limits, $V_U$ and $V_L$, respectively. The greater the number of selectable intermediate taps and capacitors stacked in series, the finer will be the variation in load voltage that can be achieved. This section explains the sequence that takes place during discharging. A similar sequence can be applied for the charging process as long as the intermediate taps of $S_0$–$S_2$ are bidirectional switches.

### 4.2.3 Experimental discharge performance

With the goal of achieving an alternative application for a 42-V-battery with an operating voltage range of 30–42 V, a 200 W discharger prototype was designed for a $V_{Load}$ of 30–40 V, a maximum load current of 5 A and an SC module at 60 V in a fully charged state. Capacitors in each SCC must be designed to be capable of RMS currents determined by the load current and switching frequency. A detailed design procedure for the capacitors has been reported elsewhere (Oraw & Ayyanar, 2007; Seeman & Sanders, 2008). The capacitances (number of capacitors) of each capacitor were determined on the basis of the reported design procedure, as shown in Table 3. Multiple ceramic capacitors were connected in parallel to satisfy the required capacitance.

| Capacitor | Capacitance |
|---|---|
| $C_1$ | 22 µF |
| $C_2$ | 44 µF (22 µF × 2) |
| $C_3$ | 44 µF (22 µF × 2) |
| $C_4$ | 110 µF (22 µF × 5) |
| $C_5$ | 66 µF (22 µF × 3) |
| $C_6$ | 22 µF |
| $C_7$ | 44 µF (22 µF × 2) |
| $C_8$ | 66 µF (22 µF × 3) |

Table 3. Capacitance of each capacitor.

A photograph of a 200 W prototype is shown in Fig. 11(a). N-channel MOSFETs with low on-resistance (9.2 mΩ for $Q_1$–$Q_6$, 1.8 mΩ for $Q_7$–$Q_{10}$) were used for switches in each SCC. The switches were operated at a fixed switching frequency of 300 kHz with 50% duty cycle.

Synchronous MOSFET gate driver ICs (ADP3120A) were used, and the ICs were powered by the stationary capacitors $C_1$–$C_3$ and $C_6$–$C_7$ via low-dropout linear regulator ICs. The intermediate taps, $S_0$–$S_2$, were composed of two MOSFETs with 9.2 mΩ on-resistance connected back-to-back.

Power conversion efficiencies when $S_0$, $S_1$ and $S_2$ were on and when $V_{Load}$ = 40 V are shown in Fig. 11(b). In the low power region, the efficiencies were relatively low because the power consumption at the MOSFET gate driver ICs accounted for a relatively large part of the input power. However, in the region above 60 W, efficiencies higher than 96% were achieved. The highest efficiency of approximately 98% was observed at 200 W.

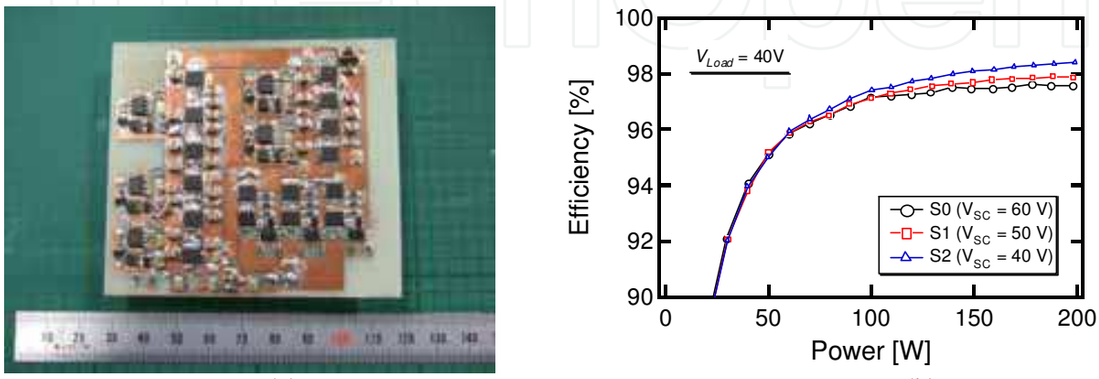


Fig. 11. (a) Photograph of a 200 W prototype and (b) power conversion efficiencies when $V_{Load}$ was 40 V.

With the prototype, an SC module with capacitance 55 F was discharged at a constant current of 4 A. The intermediate taps were shifted in the order of $S_0$, $S_1$ and $S_2$ to maintain $V_{Load}$ within 30–40 V. Experimental discharge profiles are shown in Fig. 12. The SC was discharged from 60 to 30 V while $V_{Load}$ was successfully maintained within the 30–40 V range. Discharging the SC to half of its initial voltage resulted in 75% energy utilization.

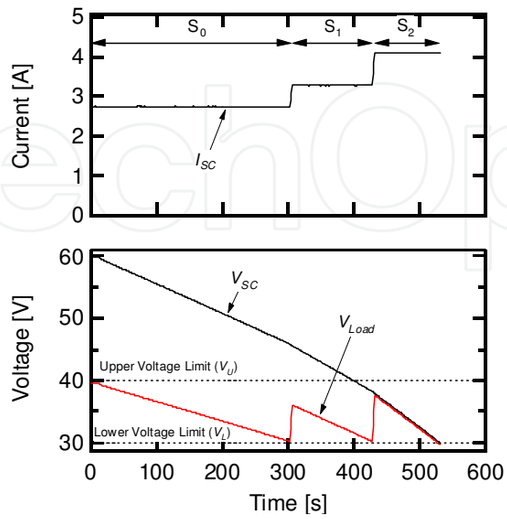


Fig. 12. Experimental discharge curves of the SC module with the prototype discharger using cascaded switched capacitor converters with selectable intermediate taps.

### 4.3 Series-parallel reconfiguration technique

#### 4.3.1 Conventional reconfiguration techniques

In conventional switching converters including the SCCs shown in the previous section, switching losses caused by high-frequency switching operations are a major factor in reducing power conversion efficiencies. Series-parallel reconfiguration techniques that do not require high-frequency switching operations have been proposed (Sugimoto, et al., 2003). Because of the negligible switching loss, the conduction loss is the only major factor affecting the efficiency; hence, these techniques achieve higher efficiencies (99.5% efficiency has been reported) than switching power converters.

Fig. 13(a) shows a series-parallel changeover circuit. Two SCs are connected in parallel at the beginning of the discharging process via $Q_1$ and $Q_2$. After the SC voltages decrease to a predetermined lower voltage level, $Q_1$ and $Q_2$ turn off, and $Q_3$ turns on to connect the SCs in series. Hence, the output voltage (load voltage) increases and the SCs can be discharged deeply. However, the voltage variation caused by the reconfiguration is as high as 50%.

Another approach employs the shift-type changeover circuit shown in Fig. 13(b). $SC_1$–$SC_2$ and $SC_3$–$SC_4$ are initially connected in parallel via $Q_1$ and $Q_2$, and hence, the whole system is two series two parallel. SC voltages decrease with discharging, and $Q_1$ and $Q_2$ turn off while $Q_3$ and $Q_5$ turn on when the SC voltages decrease to a predetermined level. At that moment, only $SC_1$ and $SC_4$ are connected in parallel while $SC_2$ and $SC_3$ are connected in series. Therefore, at this instant, the number of series connections in the entire system is three. The SC voltages decrease further with discharging, and $Q_3$ and $Q_5$ turn off, and $Q_4$ turns on. All the SCs are connected in series via $Q_4$, so the system becomes four series one parallel. This system can increase the number of series connections one by one. As a result, the voltage variation caused by the reconfiguration can be mitigated compared with the series-parallel changeover circuit shown in Fig. 13(a). However, while $Q_3$ and $Q_5$ are on, a voltage imbalance inevitably occurs because the SCs are discharged unequally (Sugimoto, et al., 2003). The unequal discharging results in poor utilization of the stored SC energies, and in the worst case, overcharging and over-discharging.

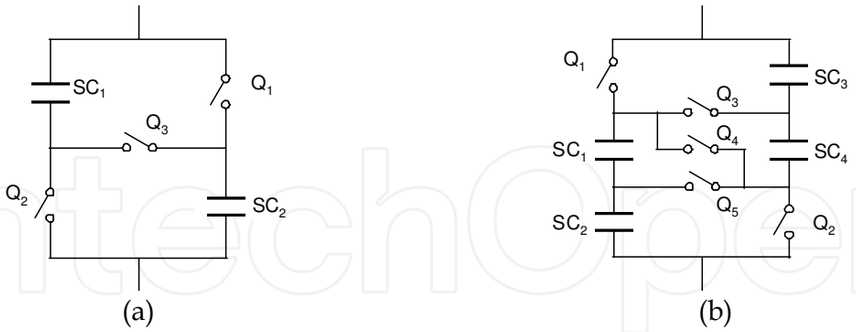


Fig. 13. Conventional reconfiguration techniques using (a) series-parallel and (b) shift-type changeover circuits.

#### 4.3.2 Series-parallel reconfigurable SC unit

Fig. 14 shows a reconfigurable series-parallel SC unit that operates in two modes, modes A and B. This unit can be used in combination with the conventional circuits shown in Fig. 13. The following experimental section presents the discharge characteristics of the SC system based on a combination of the units in Fig. 14 and the changeover circuit shown in Fig. 13(a). This section focuses on the fundamental operation of the unit in Fig. 14.

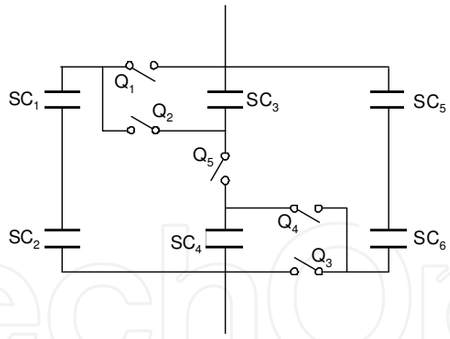


Fig. 14. Reconfigurable series-parallel SC energy storage unit.

The current flow directions and voltage curves during discharging are shown in Fig. 15. At the beginning of discharging, the unit operates as a two series three parallel system in mode A, in which three strings consisting of $SC_1$–$SC_2$, $SC_3$–$SC_4$ and $SC_5$–$SC_6$ are connected in parallel via odd-numbered switches, as shown in Fig. 15(a). As long as the capacitance of each SC is uniform, all the SCs discharge uniformly. The voltages across the SCs decrease as the discharging progresses. When the unit voltage falls below the predetermined level $V_L$, the series-parallel connections of the SC unit are reconfigured by turning off and on the odd- and even-numbered switches, respectively, as shown in Fig. 15(b).

In mode B, $SC_1$–$SC_2$ and $SC_3$, and $SC_4$ and $SC_5$–$SC_6$ are connected in series, respectively, through even-numbered switches and the unit is a three series two parallel configuration. Hence, the unit voltage at the beginning of mode B is 1.5 times higher than that at the end of mode A. In other words, the voltage variation caused by reconfiguration is 33%. This value is smaller than that for the conventional technique shown in Fig. 13(a). The unit and SC voltages in mode B decrease at a faster rate than that in mode A because of fewer parallel connections in mode B. The change in the current rate results in an inflection point in the SC voltage curve.

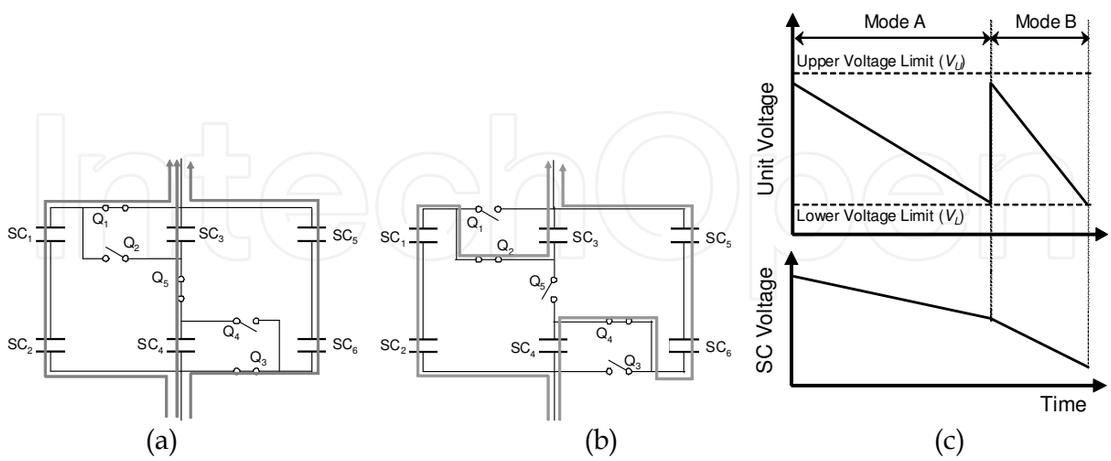


Fig. 15. Current flow directions in (a) mode A and (b) mode B, and (c) cell and unit voltage curves during discharging.

With the discharge sequence shown in Fig. 15, the SCs in the unit can be discharged deeply by reconfiguring the series-parallel configuration, while the unit voltage can be

maintained within a particular voltage range. This reconfigurable unit can achieve very high efficiencies that are similar to those of the conventional techniques because the switching loss is negligible and efficiency is only affected by the conduction losses of switches.

This section explains the operating sequence for the discharging process. A similar reconfiguration sequence can be applied to a charging process. Since the reconfigurable SC unit consists of two or three strings in parallel, the unit is considered most suitable for relatively large-scale applications where parallel connections are usually required.

### 4.3.3 Experimental discharging characteristics

An SC-based energy storage system combining the reconfigurable units shown in Fig. 14 with the changeover circuit shown in Fig. 13 is illustrated in Fig. 16(a). $SC_1$ and $SC_2$ in Fig. 13 are replaced with the unit shown in Fig. 14. The system consisting of 500 F SCs was discharged at a constant current of 1.5 A, and the resultant discharge curves are shown in Fig. 16(b). Table 4 shows the operating status of the units and switches and the system configuration during the discharging experiment.

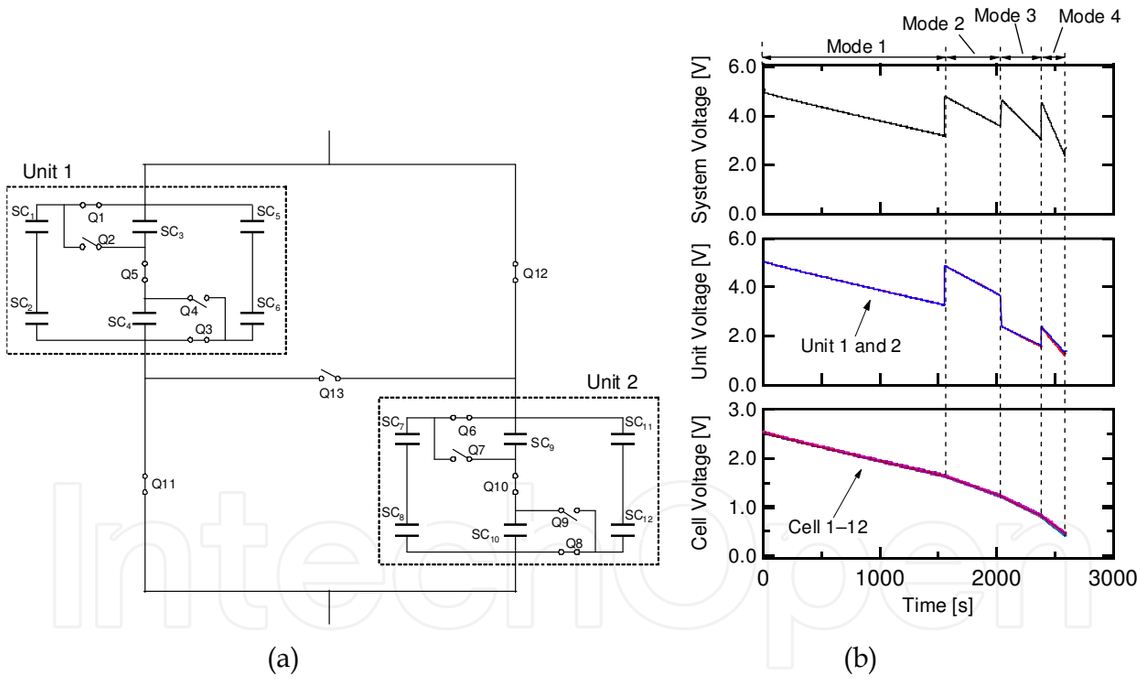


Fig. 16. (a) Reconfigurable series-parallel SC energy storage system and (b) resultant discharging curves of system, unit and cell voltages.

The system configuration was modified from mode 1 to mode 4. When a system voltage lower than a predetermined lower voltage level (approximately 3.2 V in this case) was detected, the system configuration was modified by changing the operating statuses of the units and/or switches. As the discharging progressed, the number of series connections was increased consistently, whereas the number of parallel connections was decreased. The cell voltages decreased with discharging, but the system voltage was maintained within a

desired voltage range. All the cells were uniformly and deeply discharged. The experimental results demonstrated that the system can achieve high energy utilization without causing voltage imbalance.

| | Units 1 and 2 | Q11, Q12 | Q13 | Configuration |
|---|---|---|---|---|
| Mode 1 | Mode A | ON | OFF | two series six parallel |
| Mode 2 | Mode B | ON | OFF | three series four parallel |
| Mode 3 | Mode A | OFF | ON | four series three parallel |
| Mode 4 | Mode B | OFF | ON | six series two parallel |

Table 4. Operating statuses of units and switches during discharging, and system configuration in modes 1–4.

## 5. Conclusions

SCs offer numerous benefits over traditional secondary batteries. However, SCs are usually considered to be unsuitable as main energy storage sources because of their inherent low specific energy. In addition, several major issues need to be addressed before SCs can become main energy storage sources. These include the need for cell/module voltages to be balanced and for SCs to be discharged as efficiently and deeply as possible in order to maximise the use of the stored energies.

With regards to DoD and cycle life performance, SCs can match or outperform traditional secondary batteries in terms of net specific energy. In Section 2, the potential of SCs as alternatives to secondary batteries for energy storage applications was discussed from the perspective of net specific energies and cycle life performance. SCs can be used as alternative energy storage sources to traditional secondary batteries in applications where batteries have been cycled with shallow DoDs in order to achieve long cycle lives.

In Section 3, two types of cell/module voltage equalizers that can operate with either a single switch or without a switch were presented. SC-based energy storage systems may require numerous series connections of cells/modules. Therefore, single-switch and switchless equalizers are considered to be more suitable in terms of circuit complexity, modularity, cost and reliability.

Section 4 presented two types of high-efficiency voltage converters—cascaded switched capacitor converters with selectable intermediate taps and series-parallel reconfigurable SC systems. Neither type maintains its output voltage at a constant level but the output voltage can be maintained within a desired voltage range. For the former, we experimentally demonstrated power conversion efficiencies as high as 98% at 200 W. For the latter, even higher efficiencies can be achieved since the only losses that occur are conduction losses, while switching losses are negligible.

## 6. References

Cao, J., Schofield, N. & Emadi, A. (2008). Battery Balancing Methods: A Comprehensive Review, *Proceedings of IEEE Vehicle Power and Propulsion Conference*, ISBN 978-1-4244-1848-0, Harbin, China, September 3-5, 2008

Guo, K. Z., Bo, Z. C., Gui, L. R. & Kang, C. S. (2006). Comparison and Evaluation of Charge Equalization Technique for Series Connected Batteries, *Proceedings of IEEE Applied Power Electronics Conference and Exposition*, ISBN 0-7803-9716-9, Jeju, South Korea, June 18-22, 2006

Isaacson, M. J., Hollandsworth, R. P., Giampaoli, P. J., Linkowaky, F. A., Salim, A. & Teofilo, V. L. (2000). Advanced Lithium Ion Battery Charger, *Proceedings of Battery Conference on Applications and Advances*, ISBN 0-7803-5924-0, Long Beach, California, USA, January 11-14, 2000

Kutkut, N. H., Divan, D. M. & Novotny, D. W. (1995). Charge Equalization for Series Connected Battery Strings. *IEEE Transaction on Industry Applications,* Vol. 31, No. 3, (May & June 1995), pp. 562-568, ISSN 0093-9994

Nishijima, K., Sakamoto, H. & Harada, K. (2000). A PWM Controlled Simple and High Performance Battery Balancing System, *Proceedings of IEEE Power Electronics Specialist Conference*, ISBN 0-7803-5692-6, Galway, Ireland, June 18-23, 2009

Mita, Y., Seki, S., Terada, N., Kihira, N., Takei, K. & Miyashiro, H. (2010). Accelerated Test Methods for Life Estimation of High-Power Lithium-Ion Batteries. *Electrochemistry*, Vol. 78, No. 5, pp. 384-386

Oraw, B. & Ayyanar, R. (2007). Load Adaptive, High Efficiency, Switched Capacitor Intermediate Bus Converter, *Proceedings of IEEE International Telecommunications Energy Conference*, ISBN 978-1-4244-1627-1, Rome, Italy, October 30-November 4, 2007

Pascual, C. & Krein, P. T. (1997). Switched Capacitor System for Automatic Series Battery Equalization, *Proceedings of IEEE Applied Power Electronics Conference and Exposition*, ISBN 0-7803-3704-2, Atlanta, Georgia, USA, February 23-27, 1997

Peng, F. Z., Zhang, F. & Qian, Z. (2003). A Magnetic-Less DC-DC Converter for Dual-Voltage Automotive Systems. *IEEE Transaction on Industry Applications*, Vol. 39, No. 2, (May and April 2003), pp. 511-518, ISSN 0093-9994

Seeman, M. D. & Sanders, S. R. (2008). Analysis and Optimization of Switched-Capacitor DC-DC Converters. *IEEE Transaction on Power Electronics*, Vol. 23, No. 2, (May 2008), pp. 841-851, ISSN 0885-8993

Sugimoto, S., Ogawa, S., Katsukawa, H., Mizutani, H. & Okamura, M. (2003). A Study of Series-Parallel Changeover Circuit of a Capacitor Bank for an Energy Storage System Utilizing Electric Double Layer Capacitors. *Electrical Engineering in Japan*, Vol. 145, No. 3, (November 2003), pp. 33-42

Uno, M. (2009). Interactive Charging Performance of a Series Connected Battery with Shunting Equalizers, *Proceedings of IEEE International Telecommunications Energy Conference*, ISBN 978-1-4244-2490-0, Incheon, South Korea, October 18-22, 2009

Xu, M., Sun, J. & Lee, F. C. (2006). Voltage Divider and its Application in the Two-Stage Power Architecture, *Proceedings of IEEE Applied Power Electronics Conference and Exposition*, ISBN 0-7803-9547-6, Dallas, Texas, USA, March 19-23, 2006

Yoshida, H., Imamura, N., Inoue, T., Takeda, K. and Naito, H. (2010). Verification of Life Estimation Model for Space Lithium-Ion Cells. *Electrochemistry*, Vol. 78, No. 5, pp. 482-488

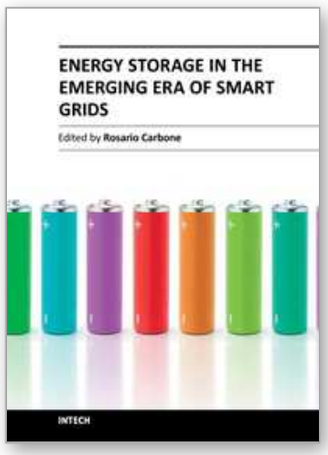


**Energy Storage in the Emerging Era of Smart Grids**

Edited by Prof. Rosario Carbone

ISBN 978-953-307-269-2
Hard cover, 478 pages
**Publisher** InTech
**Published online** 22, September, 2011
**Published in print edition** September, 2011

Reliable, high-efficient and cost-effective energy storage systems can undoubtedly play a crucial role for a large-scale integration on power systems of the emerging â€œdistributed generationâ€ (DG) and for enabling the starting and the consolidation of the new era of so called smart-grids. A non exhaustive list of benefits of the energy storage properly located on modern power systems with DG could be as follows: it can increase voltage control, frequency control and stability of power systems, it can reduce outages, it can allow the reduction of spinning reserves to meet peak power demands, it can reduce congestion on the transmission and distributions grids, it can release the stored energy when energy is most needed and expensive, it can improve power quality or service reliability for customers with high value processes or critical operations and so on. The main goal of the book is to give a date overview on: (I) basic and well proven energy storage systems, (II) recent advances on technologies for improving the effectiveness of energy storage devices, (III) practical applications of energy storage, in the emerging era of smart grids.

**How to reference**

In order to correctly reference this scholarly work, feel free to copy and paste the following:

Masatoshi Uno (2011). Supercapacitor-Based Electrical Energy Storage System, Energy Storage in the Emerging Era of Smart Grids, Prof. Rosario Carbone (Ed.), ISBN: 978-953-307-269-2, InTech, Available from: http://www.intechopen.com/books/energy-storage-in-the-emerging-era-of-smart-grids/supercapacitor-based-electrical-energy-storage-system

INTECH
open science | open minds

**InTech Europe**
University Campus STeP Ri
Slavka Krautzeka 83/A
51000 Rijeka, Croatia
Phone: +385 (51) 770 447
Fax: +385 (51) 686 166
www.intechopen.com

**InTech China**
Unit 405, Office Block, Hotel Equatorial Shanghai
No.65, Yan An Road (West), Shanghai, 200040, China
中国上海市延安西路65号上海国际贵都大饭店办公楼405单元
Phone: +86-21-62489820
Fax: +86-21-62489821

IntechOpen